

# Rapid Development and Application of Prototype Test System of Prefabricated Metro Station Structure Joint

Su Huifeng<sup>1,2,\*</sup>, Liu Weining<sup>1</sup>, Yang Xiuren<sup>3</sup> and Wang Chen<sup>3</sup>

<sup>1</sup>School of Civil Engineering, Beijing Jiaotong University, Beijing, 100044, P.R. China; <sup>2</sup>College of Transportation, Shandong University of Science and Technology, Qingdao, Shandong, 266590, P.R. China; <sup>3</sup>Beijing Urban Construction Design & Development Group Co. Limited, Beijing, 100037, P.R. China

**Abstract:** In the context of the proposed prefabricated metro station named Yuanjiadian Station for Changchun Metro Line 2 and based on the final purpose of studying the tenon and mortise grouting joint's mechanical properties, prototype test system of joint was developed and staged test finished. The test system includes loading system, test and monitoring system, assembling and grouting system, lifting and installation system and so forth. The system can complete the four-point bending test and four-point shearing test under any axial force of the prototype joint. Afterward, destructive test of axial force combining with bending moment was carried out under different conditions (including grouting ranges, grouting materials and tenon lengths). Ultimately, the flexural capacity and flexural rigidity for some specific tenon and mortise joint was derived and the safe bending moment of the joint was shown, providing guidance for design and construction.

**Keywords:** Flexural rigidity, prototype test, test system, ultimate flexural capacity.

## 1. INTRODUCTION

Recently, the proposed Yuanjiadian Station of Changchun Metro Line 2 is scheduled to take a full prefabricated structure with vertical-wall vault and column-free single arch. It will be the first total-prefabricated metro station of China. Longitudinally, seven precast blocks form one ring every two meters. One type of tenon and mortise joints with reserved space for later grouting is designed for the key circumferential and longitudinal joints. The specific form and size of the joints in different positions may be determined based on internal force, deformation and construction demand.

For the total-prefabricated structure of metro station, the most important feature is tenon and mortise grouting joints. The study of the joints' mechanical properties only by empirical model or numerical simulation does not satisfy the design requirements. The existing research of underground construction joints mostly focuses on shield segment joints, which is very different from this new one [1-8]. Given the above, joint prototype test should be conducted to study the ultimate flexural capacity, shear bearing capacity and flexural rigidity. With a view to meeting the research requirements, a feasible test system should be set up as soon as possible.

## 2. DESIGN OF TEST SYSTEM

### 2.1. Test Requirements

The test requirements are given bellow:

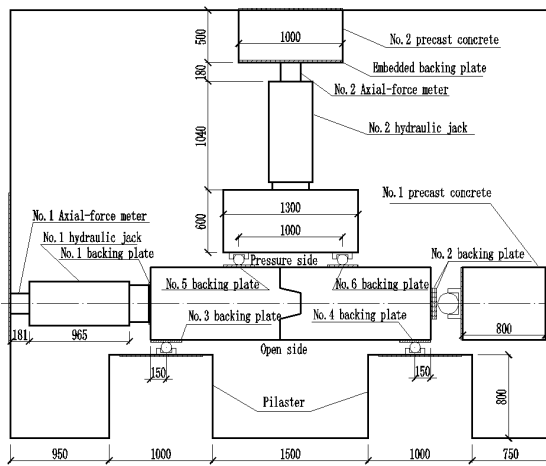
1. Transportation and hoisting of the test specimen should be convenient;
2. Enough loading space should be provided for the large-size specimen and the specimen should be conveniently installed, loaded and disassembled;
3. Any axial force test combining bending moment or shear force test can be conducted separately;
4. The loading process should be easily controlled. That is to say, the jacking speed and the load value should meet the requirements;
5. The test can be conveniently recorded;
6. The prototype test of single or double tenon and mortise joint can be done and there should be some space for other related tests;
7. A very real problem is that the test system must be built and put into use as soon as possible.

After the comparison of schemes, one scheme using the existing reaction wall and reaction frame system and the other scheme using long column machine can only complete partial test and the risk is high, so the above two schemes were abandoned. The scheme of building test-pit system in Changchun city east suburb's shield segment factory was adopted. It took 50 days from design to completion. The whole test system can be divided into loading system, monitoring system, assembling and grouting system, lifting and installation system.

### 2.2. Loading System

The length, width and height of test-pit is 7,200 mm × 5,100 mm × 1,500 mm and wall thickness 800 mm. The pit has a built-in  $\phi 25$  main reinforcement with pre-embedded 20 mm thick steel plates. Axial force and bending moment

\*Address correspondence to this author at the College of Transportation, Shandong University of Science and Technology, Qingdao, Shandong, 266590, P.R. China; Tel: +18653238961; E-mail: [shf7521@163.com](mailto:shf7521@163.com)



(a). Test-pit and single tenon and mortise joint loading arrangement



(b). Test-pit site layout

**Fig. (1).** Test-pit and single tenon and mortise joint test loading arrangement.

are provided by two horizontal hydraulic jacks separately. At the head of the jack, one universal joint is put to prevent the axial force from direction migration. Among the jacks, one provides bending moment to the test specimen *via* the distribution beam. And finally pit pilasters provide reaction. The distribution beam is made of thick steel plate with rib beam inside to offer enough stiffness. Several groups of force points are set on the beam. Vertical and axial bearings are solid steel bars with diameter of 100 mm and 200 mm respectively. The bottom of the test specimen is based with greased rollers. Between the test specimen and the bearings is a 20 mm thick steel plate to prevent the test specimen from local crushing. Within the expected load range, the loading system can meet the requirements of four-point bending test and four-point shearing test. The loading system is shown in Fig. (1).

### 2.2.1. Jack Selection

The hydraulic servo system does not only cost too much, but also requires long time to prepare and install. So it cannot be considered. Normally, the metro station is buried under a depth between 3m to 5m. So, based on the load structure theory, the internal force is obtained. In the calculation, a variety of conditions such as 0 to full rigidity of the joint stiffness was considered. The result is that the axial force is between 1,500 kN to 2,500 kN and the largest moment of the joint is 535kN.m. Considering the efficiency of the hydraulic jacks, two hydraulic jacks with rated tonnage 4000 kN and large-stroke 500 mm were selected.

### 2.2.2. Oil Pump Selection

In order to ensure the minimum jacking speed, one high-pressure fuel pump with the minimum fuel delivery of 2 L/min is selected. And the pump is equipped with constant pressure valve and digital pressure gauge. The test shows that the minimum jacking speed can be 0.28 mm/s, which is stable at the certain fuel delivery.

### 2.2.3. Force Sensor

In order for accurate measuring and real-time recording the jacking force, a high precision axial-force meter is set at

the jack tail (Brand: MTM, Type: C1-5MN, maximum range: 5000kN). It can output the practical axial force in a real time manner to the recorder (Brand: MTM, Type: 2000/CK6).

## 2.3. Monitor System Design

### 2.3.1. Static Strain Testing System

The test system is full intelligent circuit of data acquisition system named DH3816N. Each system module is equipped with 60 measuring points. Test needs 3 sets of modules and one spare.

### 2.3.2. Image and Video Collection System

Two HDTV cameras are installed on the wall of the test-pit and laboratory so as to globally and locally record the test process. At the same time, a digital camera is equipped to take photos whenever.

## 2.4. Assembling and Grouting System

For the tenon and mortise grouting joints, another important thing is the assembly of the tenon and mortise specimens and the juncture grouting. Necessary equipment such as manual hoist (rated 5t), grouting pump (maximum pressure: 0.4 MPa), level bar, water-proof slab and styrofoam are adopted.

## 2.5. Hoisting and Transportation System

According to the size and weight of the specimens, the shield segment factory's forklift (rated 10t) is used for transportation and electric hoist wheel-rail gantry crane for hoisting (rated 10t, max lifting height 2.7 m).

# 3. SPECIMENS SIZE AND MONITORING ITEM

## 3.1. Specimens Size

In the former preliminary design, the widths of the 7 joints per ring are different. The most narrow single tenon and mortise joint is 700 mm wide and the widest double tenon and mortise joint is 1,420 mm wide. The joint prototype test should be conducted conveniently and economically.

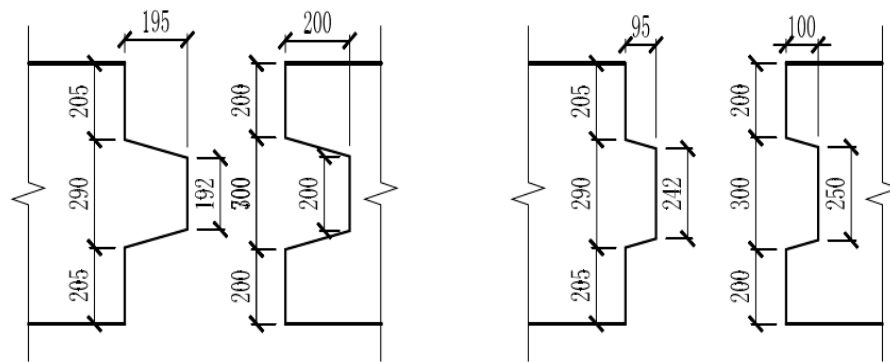
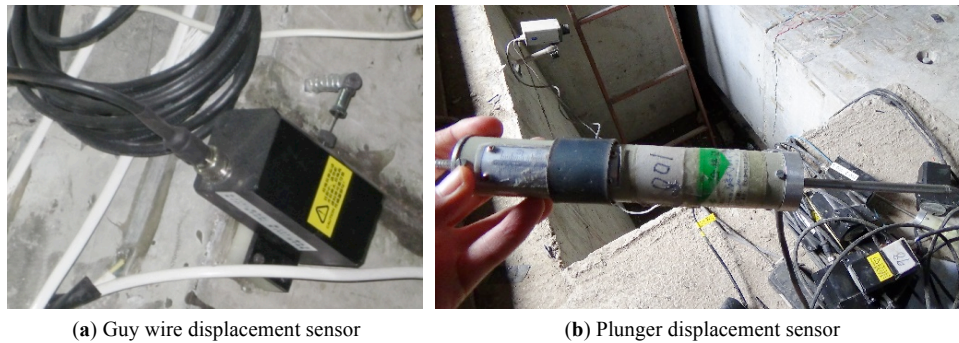


Fig. (2). Two types of single tenon and mortise specimen lengths (Unit: mm).



(a) Guy wire displacement sensor

(b) Plunger displacement sensor

Fig. (3). Two types of displacement sensors.

Table 1. The number of single tenon and mortise joint specimen’s strain gauges and displacement sensors.

Name	Concrete Strain gauge		Steel Strain gauge		Guy Wire (Plunger) Displacement Sensor
Tenon Length (mm)	195	95	195	95	195, 95
Number	70	65	44	38	9(3)

According to the principle of Saint-Venant, except a certain range of the joint designed to the real prefabricated parts, the rest is simplified into the rectangular section. The length of the assembled single tenon and mortise joint specimen is 2,700 mm and the double tenon and mortise joint is 3,600 mm long and 500 mm thick.

Section size of the single tenon and mortise joint specimen is shown in Fig. (2).

### 3.2. Joint Seam Opening Monitoring

Joint seam opening is an important index of judging the waterproof effect and flexural rigidity of the joint. Two displacement sensors such as guy wire type and plunger type were used to measure the joint seam opening. According to different measurement points, the guy wire (Type: LXW-5; Linear accuracy: superior to 1%F.S and resolving precision>0.02 mm) have two measuring ranges (50 mm and 100 mm). The plunger (Type: ZY-3770; Measuring range: 0 mm; Linear accuracy: superior to 0.5%F.S and resolving precision>0.01 mm) is convenient in measuring the joint seam opening reduction. The displacement sensors connect to the DH3816N synchronously with stress and strain and the two sensors can also check each other.

The displacement sensors are shown in Fig. (3).

### 3.3. Concrete Strain and Steel Stress Monitoring

Concrete strain and steel stress are monitored by the strain gauge. For the concrete strain monitoring, given that the small joint and its stress complexity, if the usual 100 mm strain gauges were used, it would be difficult to arrange the measuring points. Vice versa, if the strain were too short, the errors would be great. Based on the above reasons, the 50 mm concrete strain was used. For the steel strain, Type BX120-80AA was used (Table 1).

## 4. TEST APPLICATION

During the first stage, 25 single tenon and mortise specimen tests were conducted. The test involves two lengths (tenon length 195 mm and 95 mm), three types of grouting materials (epoxy, cement-based and with no grouting), three types of grouting ranges (maximum, minimum and the designed), and five axial forces (0, 500 KN, 1000 KN, 1600 KN, 2000 KN). Based on massive test data and relevant information, the single tenon and mortise joint’s flexural performance was initially obtained.



(a) Cracks developing under the condition of minimum grouting range (b) Cracks developing under the condition of designing grouting range

**Fig. (4).** Cracks developing under the condition of two grouting ranges.

**Table 2.** The key bending moment under the condition of different axial force of length 195 mm tenon.

Axial Force (kN)	Grouting Range	Cracks Appearance (kN.m)	Cracks Development (kN.m)	Cracks Cut-Through the Tenon (kN.m)	Cracks Cut-Through the Structure (kN.m)	Ultimate Bending Capacity (kN.m)
0	Minimum	55	/	72	87.5	108
500	Minimum	80	110	175	192	210
1000	Minimum	122.5	180	280	350	420
1600	Minimum	160	250	310	460	530
2000	Minimum	192	350	455	610	840

#### 4.1. Study of the Joint's Ultimate Flexural Capacity

By comparing the joint surface cracks, concrete strain, steel stress of the key position develops with the axial force and bending moment, the joint flexural capacity can be divided into several stages. Also, the safe bending moment that the joint can bear was obtained.

##### 4.1.1. Tenon Length 195 mm Specimens

The flexural capacity of the tenon 195 mm can be divided into five stages: cracks appearance, cracks development, cracks cut-through the tenon, cracks cut-through the structure and losing bearing capacity, as shown in Fig. (4). The stage before cracks cut-through the tenon should be defined as the safe bearing stage.

The bending moment for different axial forces under the condition of minimum grouting range is given in Table 2.

From Table 2, except the axial force 0, the bending moment of cracks cut-through the structure is 2.2 times of cracks appearance stage. The bending moment of cracks appearance and the edge of specimens reaching tensile strength can be obtained by simple calculation. The other conditions of the joint are the same as described above and will not be explained here.

##### 4.1.2. Tenon Length 95 mm Specimens

For the tenon 95 mm length specimens, the flexural bearing conditions are much different than the length 195 mm. The bending stages can be divided into five stages such as stage cracks appearance, stage cracks extension to the top of

the tenon, stage cracks cut-through the tenon, stage several parallel fractures appearance in groove and the final bearing stage. The stage interval after cracks appearance is too short to be distinguished (under the condition of smaller axial force), which is similar to brittle failure of the rare-reinforced beam even to plain concrete beam (Fig. 5).

The key bending moment under the condition of minimum grouting range and different axial force is given in Table 3.

For the tenon 95 mm length grouting joint, the bending moment of cracks appearance should be the maximum safe moment. As is known from mechanics, the bending moment is irrelevant to the reinforcement ratio but the size of the joint tenon.

#### 4.2. Study of the Flexural Rigidity

According to the seam opening of joints, the flexural rigidity at different times was obtained by the method of segment tangent rigidity. The flexural rigidity test formula of the joint was found suitable. Results show that flexural rigidity and bending moment have the exponential relationship. The relationship equation is as follows:

$$k_{\theta} = Ae^{\frac{B-M}{A}} \quad (1)$$

In the formula, A and B are correlation coefficients, which are related to the joint size, grouting materials, grouting range and the axial force. For the tenon 195 mm length specimen, the joint flexural rigidity formula under the condition of grouting epoxy and designing grouting range is given in Table 4.

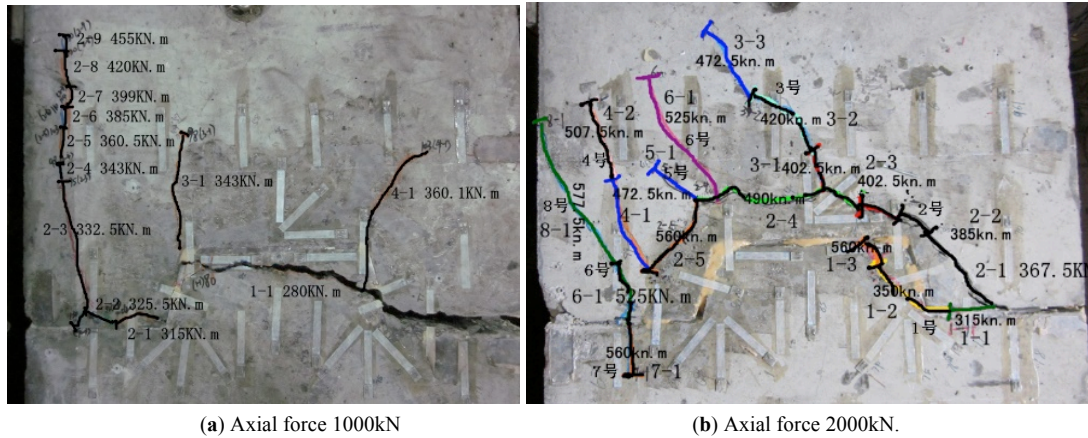


Fig. (5). Cracks developing under the condition of two axial forces.

Table 3. The key moment under the condition of minimum grouting range of tenon length 95 mm specimens.

Axial Force (kN)	Cracks Appearance (kN.m)	Cracks Extension to the Top of the Tenon (kN.m)	Cracks Cut-Through Tenon (kN.m)	Several Parallel Cracks Appearance in Groove (kN.m)	The Final Bearing (kN.m)
0	/	/	140	140	140
500	/	/	210	213.5	213.5
1000	/	/	280	280	350
1600	280	350	410	540	595
2000	315	385	490	577	665

Table 4. Joint flexural rigidity formula under the condition of grouting epoxy and designing grouting range of tenon length 195 mm specimen.

Grouting Material	Axial Force Condition (kN)	Grouting Range	Flexural Rigidity Test Formula
Epoxy	0	Design range	$k_{\theta} = 32.78e^{\frac{389.2-M}{32.78}}$
	500	Design range	$k_{\theta} = 37.03e^{\frac{459.3-M}{37.03}}$
	1000	Design range	$k_{\theta} = 68.04e^{\frac{794.3-M}{68.04}}$
	1600	Design range	$k_{\theta} = 76.43e^{\frac{879.2-M}{76.43}}$
	2000	Design range	$k_{\theta} = 101.9e^{\frac{1143-M}{101.9}}$

From Table 4, the flexural rigidity is seen to increase with the increasing axial force but decreases with the increasing moment. According to the test formula, it can be seen that the flexural behavior of 195 mm tenon joint is superior to the 95 mm one. It means that the length of the tenon has some influence on the joint flexural rigidity.

**CONCLUSION**

Some related literatures [9, 10] also describe the shield segment joint test system. But the loading tonnage and the

test items cannot be compared to the new system, and the system needs to be considered more thoroughly and more practically. Up to now, the new test system works well and test precision meets the requirements. The test data has offered a good reference for design and is also ready for the subsequent double tenons-grooves test and shear test.

**CONFLICT OF INTEREST**

The authors confirm that this article content has no conflict of interest.

**ACKNOWLEDGEMENTS**

Declared none.

**REFERENCES**

- [1] H. S. Jiang, and X.Y. Hou, "Theoretical study of rotating stiffness of joint in shield tunnel segments," *Chinese Journal of Rock Mechanics and Engineering*, vol. 23, pp. 1574-1577, 2004.
- [2] N. Yu, T.H. Bai, and H.H. Zhu, "Model experimental study on joints stiff of precast and prestressed concrete lining in shield tunnels," *Chinese Journal of Underground Space and Engineering*, vol. 5, pp. 439-449, 2009.
- [3] R. Guo, C. He, K. Feng, and M. Q. Xiao, "Bending stiffness of segment joint and its effects on segment internal force for underwater shield tunnel with large cross-section," *China Railway Science*, vol. 34, pp. 47-53, 2013.
- [4] H.E.I. Naggar, S. D. Hinchberger, and K. Y. Lo, "A closed-form solution for composite tunnel linings in a homogeneous infinite isotropic elastic medium," *Canadian Geotechnical Journal*, vol. 45, pp. 266-287, 2008.
- [5] J.G. Zhang, and C. He. "Model of mechanical behavior with whole segmental lining shield tunnel," *Engineering Mechanics*, vol. 30, pp. 136-146, 2013.
- [6] Z.X. Su, C. He. "Shell-spring-contact model for shield tunnel segmental lining analysis and its application," *Engineering Mechanics*, vol. 24, pp. 131-136, 2007.
- [7] D.Z. Zhao, and L. H. Jing, "Study on flat shell-joint element-foundation model for segment of shield tunnels," *Engineering Mechanics*, vol. 28, pp. 110-117, 2011.
- [8] J. S. Chen, and H.H. Mo, "Three-dimensional FEM analysis on flexural rigidity of segment joints in shield tunnel," *Journal of the China Railway Society*, vol. 31, pp. 87-91, 2009.
- [9] H.M. Zhan, *The Study of the Theory of the Shield Tunnel and Construction Practice*, Building Industry Press: CA: China, 2010, pp. 341-349.
- [10] M. N. Wang, Z.Y. Li, and L. H. Wei, *Tunnel and Underground Railway Precast Technology*, Southwest Jiaotong University Press: CA, 2009, pp. 1-26.

Received: June 10, 2015

Revised: July 29, 2015

Accepted: August 15, 2015

© Huifeng et al.; Licensee Bentham Open

This is an open access article licensed under the terms of the Creative Commons Attribution Non-Commercial License (<http://creativecommons.org/licenses/by-nc/4.0/>) which permits unrestricted, non-commercial use, distribution and reproduction in any medium, provided the work is properly cited.